93-GT-32

Copyright © 1993 by ASME

EFFECT OF LATERAL DISK FLEXIBILITY ON THE DYNAMICS

OF SQUEEZE FILM DAMPER SUPPORTED ROTORS

Huajun Xie
George Flowers
Fangsheng Wu

Department of Mechanical Engineering
Auburn University
Auburn, Alabama

ABSTRACT

This paper investigates the influence of disk flexibility on the dynamical behavior of a flexible disk/shaft rotor system supported with squeeze film dampers. A simplified nonlinear rotor model incorporating disk/shaft coupling dynamics is developed for lateral vibration of a rotor system. The steady state performance of the system is explored over a wide range of operating conditions using numerical integration and harmonic balance analysis. It is shown that disk flexibility may significantly affect the dynamical behavior of the system at high operating speed by creating an additional critical speed. It is observed that both the SFD journal motion and the disk motion associated with the additional critical speed are aperiodic and of large amplitudes. It is demonstrated that the influence of disk flexibility can be shifted out of the operating speed range by increasing the retainer spring stiffness.

NOMENCLATURE

A_R = coefficient of radial fluid film force
A_T = coefficient of tangential fluid film force
$B_k = \mu R L^3/(C^3 m \omega_r)$ bearing parameter of SFD
C = radial clearance of SFD
e = journal eccentricity
F_1 = fluid film force in the x_1 direction
F_2 = fluid film force in the x_2 direction
I_h = inertia of rotor hub
L = axial length of SFD
L_s = rotor shaft length
m = half of rotor mass
m_d = one-fourth of disk mass

$m_1 = 2I_b/L_s^2 + 4m_d r^2/L_s^2 + m$
$m_2 = r m_d/L_s$
$m_3 = 8m_d r^2/L_s^2$
$m_{20} = m_2/m_d$
$m_{21} = m_2/m_1$
$m_{31} = m_3/m_1$
N = number of harmonics
R = bearing radius of SFD
r = disk radius
T = transmissibility
$U = u/C$ imbalance parameter
u = static imbalance
x_1, x_2 = shaft degrees of freedom
x_3, x_4 = disk degrees of freedom
z_1, z_2, z_3, z_4 = physical displacements for disk mass elements
μ = absolute viscosity of lubricant
$\Lambda_1 = \omega_r/\Omega$
$\Lambda_2 = \omega_d/\Omega$
Ω = rotor speed
ω = design speed of the rotor
ω_d = natural frequency of the non-rotating disk
ω_r = natural frequency of the retainer spring-rotor system
$\bar{\omega}_s = \omega_r/\omega$ spring parameter
ψ_i = azimuth angle for ith disk mass
ζ = damping ratio for the disk
$\tau = \Omega t$
$(') = d/d\tau$

INTRODUCTION

Squeeze film dampers can provide significant attenuation of rotor vibration amplitudes and improved rotor stability

if appropriately designed. Great efforts have been made over the years to investigate the effects of various system parameters on the performance of squeeze film damper supported rotors. A number of important studies on this topic are available in the technical literature. Those that have most influenced the current work are discussed below. Mohan and Hahn (1974) and Rabinowitz and Hahn (1977a) studied the steady state performance of squeeze film damper supported rotors for design purposes. San Andres and Vance (1986), Tichy (1987) and El-Shafei (1988) investigated the effects of fluid inertia. Feng (1988) and Zeidan and Vance (1990) examined cavitation effects. Rabinowitz and Hahn (1977b) and Sato et al. (1991) discussed stability characteristics.

To the authors' knowledge, all of the work related to squeeze film damper supported rotors has either explicitly or implicitly assumed that any disks attached to the shaft are rigid, neglecting the coupling between the dynamics of the disk and that of the shaft. Such an assumption is adequate in applications where disks are designed to be very rigid and disk flexibility is indeed negligible. However, in many applications, especially in modern aircraft engines, flexible disks are common due to the trend in design toward higher speeds and lower weight (Klompas, 1974 and Chivens and Nelson, 1975). Studies of rotor models in which the effects of disk flexibility have been included indicate that it may significantly alter rotordynamical behavior under certain conditions (Vance, 1988 and Wilgen and Schlack, Jr., 1979). Since modern aircraft engines typically utilize squeeze film dampers in conjunction with rolling element bearings, it is important to study what effects disk flexibility might have on the performance of squeeze film damper supported rotors.

This paper is concerned with the dynamics of a flexible disk/shaft rotor system supported with squeeze film dampers. The steady state responses of the system are investigated using harmonic balance analysis and numerical integration.

THEORETICAL MODEL

The theoretical model in this investigation is largely based on the work of Flowers and Wu (1992). A schematic diagram of the model is shown in Fig. 1. The disk is modelled as a collection of four equally spaced mass elements connected to a central hub by linear springs. The rigid central hub simulates the shaft/disk interconnection. The equation development for this model is based on the following assumptions: (1) the shaft is rigid and symmetric; (2) the hub is restricted to have only rotational motion; (3) the disk motion is assumed to be asymmetrical around the circumference of the disk; (To be specific, this assumption means that $z_1 = -z_3$ and $z_2 = -z_4$. This kind of motion
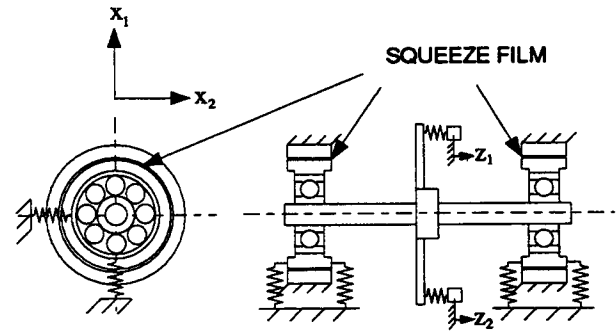

FIG. 1 SCHEMATIC DIAGRAM OF THE MODEL

results in responses that transmit a moment to the shaft and thereby assures that the disk motion and the shaft motion are coupled.) (4) π–film short bearing approximation is valid for the squeeze film dampers; (5) the rotor is centrally preloaded with retainers of constant symmetric radial stiffness; (6) the rotor speed is constant; (7) the Reynolds equation for constant fluid properties is applicable and the pressures at the ends of the damper are ambient; (8) the fluid inertia forces are neglected.

The equations of motion that result are:

$$x_1'' - m_{21}x_3'' - 2m_{21}x_4' + m_{31}x_2'$$
$$+\Lambda_1^2 x_1 - F_1 = u\,cos(\Omega t) \qquad (1.a)$$

$$x_2'' - m_{21}x_4'' + 2m_{21}x_3' - m_{31}x_1'$$
$$+\Lambda_1^2 x_2 - F_2 = -u\,sin(\Omega t) \qquad (1.b)$$

$$-4m_{20}x_1''+x_3'' - 8m_{20}x_2' + 2x_4' - x_3$$
$$+\Lambda_2^2 x_3 + 2\zeta\Lambda_2 x_3' = 0 \qquad (1.c)$$

$$-4m_{20}x_2''+x_4'' + 8m_{20}x_1' - 2x_3' - x_4$$
$$+\Lambda_2^2 x_4 + 2\zeta\Lambda_2 x_4' = 0 \qquad (1.d)$$

where

$$x_3 = \sum_{i=1}^{4} z_i cos(\Omega t + \psi_i)$$

$$x_4 = \sum_{i=1}^{4} z_i sin(\Omega t + \psi_i)$$

2

In the above equations, F_1 and F_2 are derived from the dynamic fluid force expressions for π–film short bearings given by Vance (1988).

$$F_1 = -\frac{\Lambda_1 B_k C^3 (A_T x_2 + A_R x_1)}{\sqrt{x_1^2 + x_2^2}(C^2 - x_1^2 - x_2^2)^2} \qquad (2.a)$$

$$F_2 = -\frac{\Lambda_1 B_k C^3 (A_R x_2 - A_T x_1)}{\sqrt{x_1^2 + x_2^2}(C^2 - x_1^2 - x_2^2)^2} \qquad (2.b)$$

where

$$A_R = \frac{\pi(C^2 + 2x_1^2 + 2x_2^2)(x_1 x_1' + x_2 x_2')}{2\sqrt{(C^2 - x_1^2 - x_2^2)(x_1^2 + x_2^2)}} + 2|x_1' x_2 - x_1 x_2'|$$

$$A_T = \frac{\pi(x_1' x_2 - x_1 x_2')\sqrt{C^2 - x_1^2 - x_2^2}}{2\sqrt{x_1^2 + x_2^2}} - 2(x_1 x_1' + x_2 x_2')$$

For steady-state motion, it is assumed that the squeeze film damper executes a circular centered orbit motion. Thus, F_1 and F_2 can be simplified and expressed in the following forms:

$$F_1 = -\frac{\Lambda_1 B_k C^3 (A_T x_2 + A_R x_1)}{\sqrt{x_1^2 + x_2^2}} \qquad (3.a)$$

$$F_2 = -\frac{\Lambda_1 B_k C^3 (A_R x_2 - A_T x_1)}{\sqrt{x_1^2 + x_2^2}} \qquad (3.b)$$

where

$$A_R = \frac{2|x_1' x_2 - x_1 x_2'|}{(C^2 - x_1^2 - x_2^2)^2}$$

$$A_T = \frac{\pi(x_1' x_2 - x_1 x_2')}{2\sqrt{x_1^2 + x_2^2}(C^2 - x_1^2 - x_2^2)^{3/2}}$$

ANALYSIS

Since the current research work is primarily concerned with periodic motions, the harmonic balance method is used to study the dynamic responses. To apply the harmonic balance method, the steady-state responses associated with equations (1) and the nonlinear SFD fluid forces expressed in equations (3) are assumed to have the following forms:

$$x_j = \sum_{i=1}^{N}[a_{ji}cos(k_i\Omega t) + b_{ji}sin(k_i\Omega t)] \qquad (4.a)$$

$$(j = 1, 2, 3, 4)$$

$$F_1 = \sum_{i=1}^{N}[(g_{1i}cos(k_i\Omega t) + h_{1i}sin(k_i\Omega t)] \qquad (4.b)$$

$$F_2 = \sum_{i=1}^{N}[(g_{2i}cos(k_i\Omega t) + h_{2i}sin(k_i\Omega t)] \qquad (4.c)$$

Substituting equations (4) into the equations of motion (1) and equating all the trigonometric terms, we obtain the following nonlinear algebraic equations in matrix form:

$$A_i P_{1i} + B_i P_{2i} - Q_i - F_i = 0 \qquad (5.a)$$

$$C_i P_{1i} + D_i P_{2i} = 0 \qquad (5.b)$$

where

$$A_i = \begin{pmatrix} -k_i^2 + \Lambda_1^2 & 0 & 0 & m_{31}k_i \\ 0 & -k_i^2 + \Lambda_1^2 & -m_{31}k_i & 0 \\ 0 & -m_{31}k_i & -k_i^2 + \Lambda_1^2 & 0 \\ m_{31}k_i & 0 & 0 & -k_i^2 + \Lambda_1^2 \end{pmatrix}$$

$$B_i = \begin{pmatrix} m_{21}k_i^2 & 0 & 0 & -2m_{21}k_i \\ 0 & m_{21}k_i^2 & 2m_{21}k_i & 0 \\ 0 & 2m_{21}k_i & m_{21}k_i^2 & 0 \\ -2m_{21}k_i & 0 & 0 & m_{21}k_i^2 \end{pmatrix}$$

$$C_i = \begin{pmatrix} 4m_{20}k_i^2 & 0 & 0 & -8m_{20}k_i \\ 0 & 4m_{20}k_i^2 & 8m_{20}k_i & 0 \\ 0 & 8m_{20}k_i & 4m_{20}k_i^2 & 0 \\ -8m_{20}k_i & 0 & 0 & 4m_{20}k_i^2 \end{pmatrix}$$

$$D_i =$$

$$\begin{pmatrix} \Lambda_2^2 - 1 - k_i^2 & 2\zeta\Lambda_2 k_i & 0 & 2k_i \\ -2\zeta\Lambda_2 k_i & \Lambda_2^2 - 1 - k_i^2 & -2k_i & 0 \\ 0 & -2k_i & \Lambda_2^2 - 1 - k_i^2 & 2\zeta\Lambda_2 k_i \\ 2k_i & 0 & -2\zeta\Lambda_2 k_i & \Lambda_2^2 - 1 - k_i^2 \end{pmatrix}$$

$$P_{1i} = \begin{pmatrix} a_{1i} \\ b_{1i} \\ a_{2i} \\ b_{2i} \end{pmatrix} \qquad P_{2i} = \begin{pmatrix} a_{3i} \\ b_{3i} \\ a_{4i} \\ b_{4i} \end{pmatrix}$$

$$Q_i = \begin{pmatrix} g_{1i} \\ h_{1i} \\ g_{2i} \\ h_{2i} \end{pmatrix} \qquad F_i = \begin{pmatrix} \delta F_u \\ 0 \\ 0 \\ -\delta F_u \end{pmatrix}$$

where

$$\delta = 1 \quad \text{if} \quad k_i = 1$$
$$\delta = 0 \quad \text{if} \quad k_i \neq 1$$

Rearrangement of equation (5.b) yields:

$$P_{2i} = -D_i^{-1} C_i P_{1i} \qquad (6)$$

Substituting the above expression for P_{2i} into equation (5.a) results in the following expression:

$$(A_i - B_i D_i^{-1} C_i) P_{1i} - Q_i - F_i = 0 \qquad (i = 1, ..., N) \quad (7)$$

Equation (7) is a nonlinear algebraic equation in terms of the unknown constants associated with the assumed responses. Q is a nonlinear function of P_1. In this study, an IMSL (Version 1.1) routine based on the Levenberg-Marquardt algorithm is used to solve equation (7) for the unknown constants.

DISCUSSION OF RESULTS

Parametric studies were performed for varied imbalance parameter U, retainer spring parameter $\bar{\omega}_s$, and bearing clearance C, respectively. In order to avoid excessive cluttering of the figures with parametric plots, typical results from each type will be presented and discussed. The nominal parametric configration concerning the disk flexibility and the system mass distributions is listed in Table 1. The parameters selected for the example cases are based on current literature in this area and are thought to be representative values. Specifically, three values, $\omega_d = 0.4$, $\omega_d = 0.5$ and $\omega_d = 0.6$, were chosen to represent different degrees of disk flexibility for the case of flexible disk. The SFD radial clerance C was varied from 0.001 in. to 0.01 in. during the analysis. The results obtained for all values of C within this range are almost identical. The results presented in this paper are for the case of $C = 0.001$ in.. The reason for choosing this C value is to make it sufficiently small such that the assumption that the fluid inertia force of the SFD is negligible is valid.

Figs. 2(a)-2(b) are the predicted imbalance responses of the SFD journal. Since synchronous responses are assumed for the steady-state motion, the results presented here are obtained from the first harmonic only. It is seen that the disk flexibility can significantly affect the dynamical behavior of the system at high operating speed. In fact, an additional critical speed within the operating speed range can be created by the disk flexibility. This phenomenon was also observed in an earlier investigation (Wu and Flowers, 1992). As is shown, this critical speed is exclusively dependent on the disk flexibility. As the disk flexibility decreases (or ω_d increases),
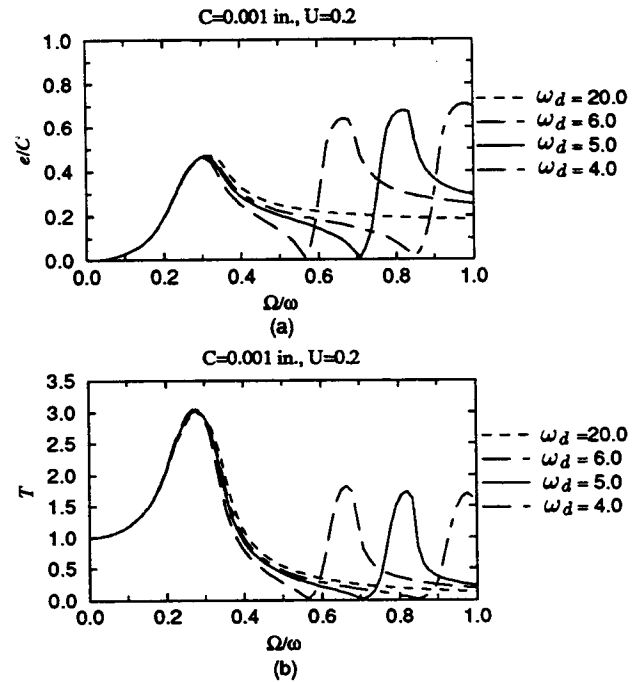

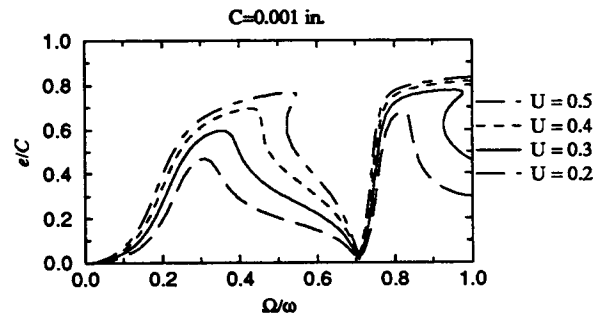FIG. 2 EFFECT OF DISK FLEXIBILITY ON ROTOR RESPONSES ($\bar{\omega}_s = 0.283$)

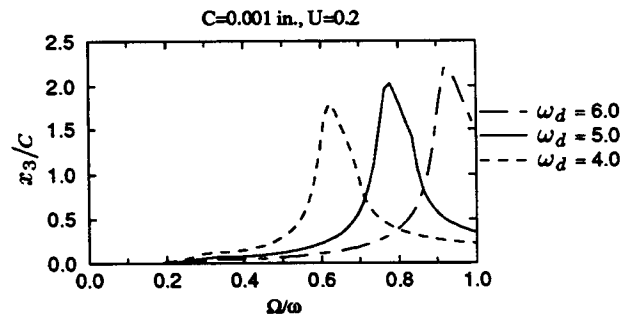FIG. 3 IMBALANCE RESPONSE OF SFD JOURNAL ($\bar{\omega}_s = 0.283$, $\omega_d = 5.0$)

FIG. 4 IMBALANCE RESPONSE OF THE DISK ($\bar{\omega}_s = 0.283$)

4

TABLE 1. NOMINAL PARAMETER VALUES

Parameter	Value	Parameter	Value
ω_r	1.0	m_{20}	0.2
ω_d	5.0	m_{21}	0.1
$\bar{\omega}_s$	0.283	m_{31}	0.16
ζ	0.01	C	0.001 in.

the additional critical speed increases. If the disk flexibility becomes sufficiently low (that is ω_d becomes larger than a certain value), the additional critical speed vanishes. On the other hand, the whirling amplitudes corresponding to this additional critical speed are even greater than those corresponding to the first critical speed associated with the natural frequency of the rotor ω_r. It is observed that the disk flexibility also produces a dip on the imbalance response curve. That is, after the operating speed has passed the first critical speed, the journal whirling amplitude gradually drops to zero and then increases again as the speed increases. The cause of this dip phenomenon will be discussed in the next paragraph. Fig. 3 shows the influence of the imbalance parameter U on the journal responses with $\omega_d = 0.5$. It is noted that the dominant effect of disk flexibility is basically independent of the imbalance parameter U for a certain SFD design configuration. However, large values of imbalance can cause multi-valued responses and, as always, large whirling amplitudes. As is expected, the dominant influence of disk flexibility at high operating speed is due to the resonant motion of the disk. This can be clearly seen from Fig. 4.

To verify the results obtained from the harmonic balance analysis, simulation studies are performed at selected points through numerical integration of the governing differential equations (1). Because the simulation process includes the transient responses, the steady-state forms of the SFD fluid forces of equations (3) are no longer valid. Therefore, equations (2) are used instead. Figs. 5(a)-5(d) are typical simulation results for the case of C=0.001 in. and U=0.2, which corresponds to the curve of ω_d=5.0 of Fig. 2(a). It is seen that at low operating speed, the SFD journal motion and the disk motion are 180° out of phase. Actually, this is the case for all the operating speed below that corresponding to the smallest amplitude on the response curve ($\Omega/\omega < 0.71$ for this example). As the speed increases, the disk motion becomes larger, gradually approaching the resonant amplitude. At the speed corresponding to the smallest amplitude, the journal motion and the disk motion are 90° out of phase. As the operating speed continues to increase, the disk natural frequency is excited and the journal motion and the disk motion become in phase. This kind of phase changes were also noticed in another earlier investigation (Flowers, 1990). More importantly, at this stage, both the journal motion and the disk motion become aperiodic. It should be pointed out that because of the motion is no
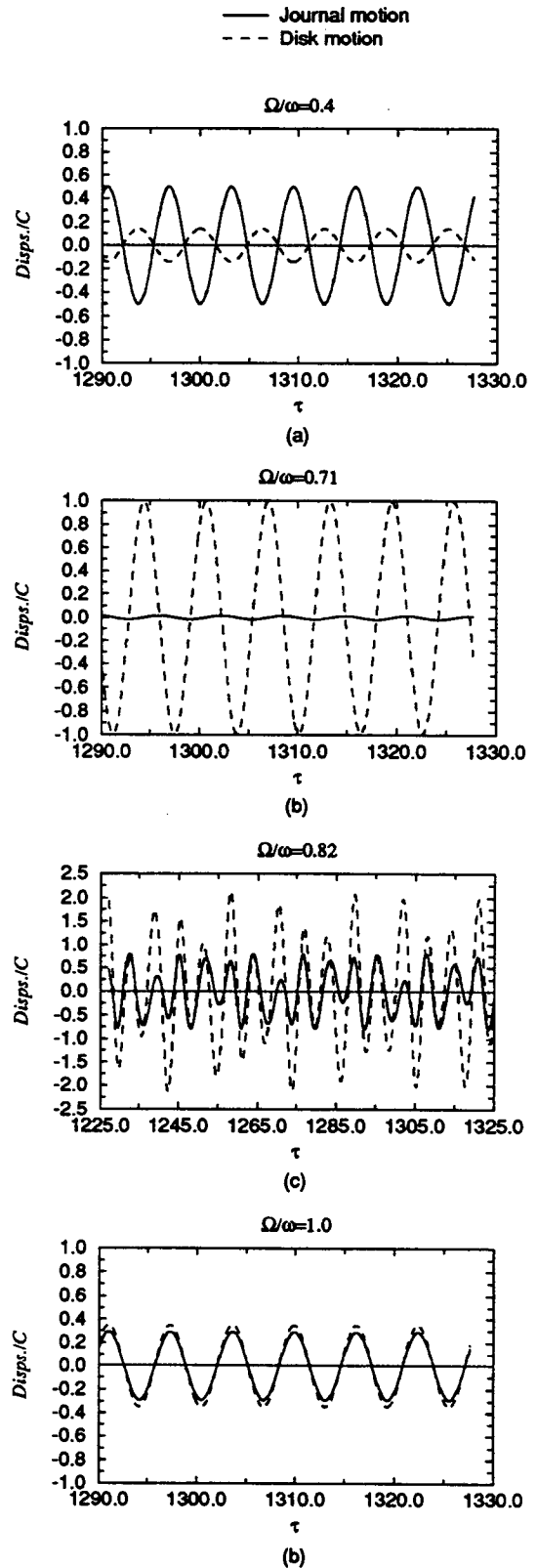

FIG. 5   SIMULATIONS OF ROTOR RESPONSES
($\omega_d = 5.0$, $\bar{\omega}_s = 0.283$, $C = 0.001 in.$)

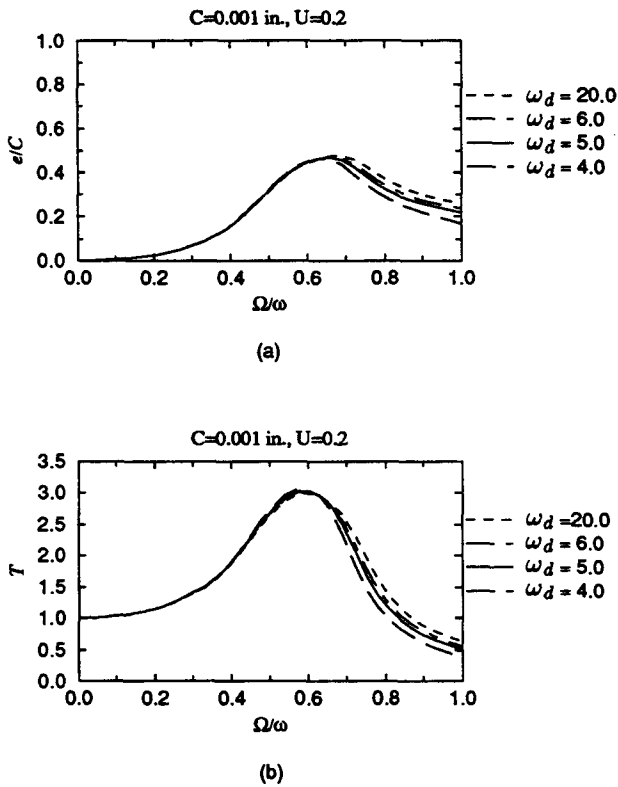## C=0.001 in., U=0.2

(a)

C=0.001 in., U=0.2

(b)

FIG. 6 EFFECT OF DISK FLEXIBILITY ON ROTOR RESPONSES ($\bar{\omega}_s = 0.6$)

longer periodic at high operating speed, the amplitude values associated with high operating speeds shown in Fig. 2(a) are not real radii of whirling orbits, but approximate radii of the first harmonics.

Figs. 6(a)-6(b) demonstrate the benefit of increased values of spring parameters $\bar{\omega}_s$. It is seen that the dominant range of disk flexibility can be shifted beyond the design operating speed by increasing $\bar{\omega}_s$ to a certain value. However, there is a penalty associated with large values of $\bar{\omega}_s$. As is well known, the transmissibility T increases with increasing values of $\bar{\omega}_s$. Therefore, compromises have to be made in choosing the optimal value of $\bar{\omega}_s$ for a certain design configuration.

CONCLUSIONS

This investigation has shown that disk flexibility may significantly influence the dynamical behavior of a squeeze film damper supported flexible disk/shaft rotor system if the stiffness of the disk is below a certain value. Of particular interests is the appearance of an additional critical speed within the operating speed range. The phase between the SFD journal motion and the disk motion changes with operating speed from completely out of phase to totally in phase.

As a brief summary, the following results were observed in this investigation:

1. Disk flexibility can producing an additional critical speed within the operating speed range.
2. Both the journal motion and the disk motion associated with the additional critical speed are aperiodic and of large amplitudes.
3. The additional critical speed can be shifted beyond the operating speed range by increasing the retainer spring stiffness to a certain value.
4. At low operating speed, the journal motion and the disk motion are 180° out of phase. As the speed increases, the two motions become 90° out of phase. After the operating speed has passed the additional critical speed, the two motions become in phase.
5. The dominant effect of disk flexibility is basically independent of the imbalance parameter U for a certain design configuration. However, large imbalance may result in multivalued responses.

ACKNOWLEDGEMENT

REFERENCES

Chivens, D. R., and Nelson, H. D., 1975, "The Natural Frequencies and Critical Speeds of Rotating, Flexible Shaft-Disk System," ASME *Journal of Engineering for Industry*, Vol. 97, pp. 881-886.

El-Shafei, A., 1988, "Dynamics of Rotors Incorporating Squeeze Film Dampers," Ph.D. Thesis, Massachusetts Institute of Technology, Cambridge, MA.

Flowers, G. T., 1990, "Effects of Rotor Disk Flexibility on the Rotordynamics of the Space Shuttle Main Engine Turbopumps," *Proceedings of the 31st AIAA/ASME/ASCE /AHS/ASC Structural Dynamics and Materials Conference*, Part 1, pp. 2206-2213.

Flowers, G. T., and Wu, F., 1992, "A study of the Influence of Bearing Clearance on Lateral Coupled Shaft/Disk Rotordynamics," to appear in ASME *Journal of Turbomachinery*, accepted for publication February, 1992.

Klompas, K., 1974, "Theory of Rotor Dynamics with Coupling of Disk and Blade Flexibility and Support Structure Asymmetry," ASME Paper 74-GT-159.

Mohan, S., and Hahn, E. J., 1974, "Design of Squeeze Film Damper Supports for Rigid Rotors," ASME *Journal of Engineering for Industry*, Vol. 96, pp. 976-982.

Rabinowitz, M. D., and Hahn, E. J., 1977a, "Steady-State Performance of Squeeze Film Damper Supported Flexible Rotors," ASME *Journal of Engineering for Power*, Vol. 99, pp. 552–558.

Rabinowitz, M. D., and Hahn, E. J., 1977b, "Stability of Squeeze Film Damper Supported Flexible Rotors," ASME *Journal of Engineering for Power*, Vol. 99, pp. 545–551.

San Andres, L. A., and Vance, J. M., "Effect of Fluid Inertia on the Performance of Squeeze Film Damper Supported Rotors," ASME *Journal of Engineering for Gas Turbines and Power*, Vol. 110, pp. 51–57.

Sato, Y., Fujino, H., Sakakida, H., and Hisa, S., 1991, "Stability Characteristics of a Journal Bearing Mounted in an Uncentralized Squeeze Film Damper," ASME *Journal of Tribology*, Vol. 113, pp. 584–589.

Tichy, J. A., 1987, "A Study of the Effect of Fluid Inertia and End Leakage in the Finite Squeeze Film Damper," ASME *Journal of Tribology*, Vol. 109, pp. 54–59.

Vance, J. M., 1988, "Rotordynamics of Turbomachinery," John Wiley & Sons, Inc., New York, NY.

Wilgen, F. J., and Schlack, Jr., A. L., "Effects of Disk Flexibility on Shaft Whirling Stability," ASME *Journal of Mechanical Design*, Vol. 101, pp. 298-303.

Wu, F., and Flowers, G. T., 1992, "A Transfer Matrix Technique for Evaluating the Natural Frequencies and Critical Speeds of a Rotor With Multiple Flexible Disks," ASME *Journal of Vibration and Acoustics*, Vol. 114, pp. 242-248.

Zeidan, F., and Vance, J., 1990, "Cavitation and Air Entrainment Effects on the Response of Squeeze Film Supported Rotors," ASME *Journal of Tribology*, Vol. 112, pp. 347–353.

7